ehp ENVIRONMENTAL HEALTH PERSPECTIVES

ehponline.org

Exposure of Rats to Environmental Tobacco Smoke during Cerebellar Development Alters Behavior and Perturbs Mitochondrial Energetics

Brian F. Fuller, Diego F. Cortes, Miranda K. Landis, Hiyab Yohannes, Hailey E. Griffin, Jillian E. Stafflinger, M. Scott Bowers, Mark H. Lewis, Michael A. Fox and Andrew K. Ottens

http://dx.doi.org/10.1289/ehp.1104857

Online 26 September 2012

NIEHS
National Institute of Environmental Health Sciences

National Institutes of Health
U.S. Department of Health and Human Services

Exposure of Rats to Environmental Tobacco Smoke during Cerebellar Development Alters Behavior and Perturbs Mitochondrial Energetics

Brian F. Fuller[1,2], Diego F. Cortes[1], Miranda K. Landis[1], Hiyab Yohannes[1], Hailey E. Griffin[1], Jillian E. Stafflinger[1], M. Scott Bowers[3], Mark H. Lewis[4], Michael A. Fox[1] and Andrew K. Ottens[1,2]*

[1]Departments of Anatomy & Neurobiology, Virginia Commonwealth University, Richmond, Virginia, USA

[2]Departments of Biochemistry and Molecular Biology, Virginia Commonwealth University, Richmond, Virginia, USA

[3]Department of Psychiatry, Virginia Institute of Psychiatric and Behavioral Genetics, Virginia Commonwealth University, Richmond, Virginia, USA

[4]Department of Psychiatry, McKnight Brain Institute of the University of Florida, Gainesville, Florida, USA

***Corresponding Author:**

Andrew K. Ottens, Ph.D.

Department of Anatomy and Neurobiology

Virginia Commonwealth University

PO Box 980709, Richmond, VA, 23298-0709.

Tel:804-628-2972; Fax:804-828-9477; Email:akottens@vcu.edu

Running Title: Postnatal ETS perturbation of Mitochondria

Key Words

Attention deficit/hyperactivity disorder, Carbohydrate metabolism, Cerebellum, Environmental tobacco smoke, Mitochondrial biogenesis, Mitochondrial energetics, Neurodevelopment, Proteomics, Secondhand smoke, Systems biology

ACKNOWLEDGEMENTS

We are grateful for assistance from: Y. Tanimura and B. McLaurin with animal handling; R. Hamm for behavioral testing; A. Lichtman and S. O'Neal for the use of ANY-Maze system, S. Geromanos, H. Vissers and M. Gorenstein for informatics; J. Williamson, S. Henderson, P. Trimmer, L. Phillips and T. Reeves, and T. Smith for electron microscopy, performed at the VCU Department of Anatomy and Neurobiology Microscopy Facility, supported with funding from NIH-NINDS grant NS047463. The authors declare that they have no competing financial interests. This research was supported in part by NIH-NINDS grant NS055012.

Abbreviations

ADHD	attention deficit hyperactivity disorder
ATP5	ATP synthase
CD	conduct disorder
CNT	control
Dnm1l	dynamin-1-like protein
ETS	environmental tobacco smoke
GL	granular layer
Hk1	hexokinase 1
ML	molecular layer
PL	Purkinje layer
TSP	total suspended particulate

ABSTRACT

BACKGROUND: Environmental tobacco smoke exposure, ETS, is linked to developmental deficits and disorders with known cerebellar involvement. However, a direct biological effect and underlying neurochemical mechanisms remain unclear.

OBJECTIVES: Our study sought to address underlying neurochemical change in the rat cerebellum with ETS exposure during critical period development.

METHODS: We exposed rats to daily ETS (300, 100 and 0 $\mu g/m^3$ *TSP*) from postnatal day 8 (P8) to P23. We assayed behavioral, neuroproteomic and cellular change in response to postnatal ETS exposure.

RESULTS: Postnatal ETS exposure induced heightened locomotor response in a novel environment on par initially with amphetamine stimulation. The cerebellar mitochondrial subproteome was significantly perturbed in the ETS exposed rats. Findings revealed a dose-dependent upregulation of aerobic processes through modification and increased translocation of Hk1 to the mitochondrion with heightened ATP5 expression. ETS exposure also induced a dose-dependent increase in total Dnm1l mitochondrial fission factor; though, more active membrane bound Dnm1l was found at the lower dose. Dnm1l activation was associated with greater mitochondrial staining, particularly in the molecular layer, which was independent of stress-induced Bcl-2 family dynamics. Further, electron microscopy associated Dnm1l-mediated mitochondrial fission with increased biogenesis, rather than fragmentation.

CONCLUSIONS: The critical postnatal period of cerebellar development is vulnerable to the effects of ETS exposure resulting in altered behavior. The biological effect of ETS is underlain in part by a Dnm1l-mediated mitochondrial energetic response at a time of normally tight control. These findings represent a novel mechanism by which environmental exposure can impact neurodevelopment and function.

INTRODUCTION

Recent epidemiological studies find a dose-dependent increased risk for behavioral and cognitive problems and a greater incidence of mental disorders in children exposed to environmental tobacco smoke (ETS) (Anderko et al. 2010; Bandiera et al. 2011; Kabir et al. 2011). Confirming earlier findings, these works address two major concerns highlighted in the U.S. Surgeon General report on ETS health consequences by employing objective biomarker measurements and determining that effects are independent of maternal smoking (U.S. Department of Health and Human Services 2006). Thus, nearly one-in-five U.S. children are at greater risk for mental health problems due to postnatal ETS exposure, a prevalence that has remained unchanged for over a decade (Centers for Disease Control and Prevention. 2010). ETS exposure is more pronounced in the young due to higher respiration rates and 50% of mothers who cease smoking during pregnancy resume in under six months post-term (Colman and Joyce 2003; Marano et al. 2009). The issue is of even greater concern worldwide, with over 50% of children regularly exposed to ETS across large parts of Europe and Asia (Oberg et al. 2011). Yet, it remains undetermined whether early ETS exposure directly affects neurodevelopment to induce behavioral change and what biological mechanisms might underlie its effects.

Activity, attention, impulsivity and language deficits reported with greater incidence in ETS exposed children all involve cerebellar regulation through feedback loops to the neocortex (Bledsoe et al. 2011; O'Halloran et al. 2012; Richter et al. 2005). Reduced cerebellar size and function have also been associated with attention deficit hyperactivity disorder (ADHD) and conduct disorders (CD) (Aguiar et al. 2010; Dalwani et al. 2011; O'Halloran et al. 2012; Richter

et al. 2005). A meta analysis of ADHD structural imaging studies found reproducible cerebellar abnormalities in posterior cerebellum such as in lobule VIII (Valera et al. 2007). Cerebellum vulnerability may be linked with its distinct late development for mammals, including humans. Research by Dobbing et al. established the precept of a vulnerable period for neurodevelopment as reviewed elsewhere (Dobbing 1982), which in the human cerebellar-cortex extends more than a year after birth rendering it susceptible to postnatal ETS effects (Dobbing 1982; Friede 1973; Koop et al. 1986). Corresponding rat cerebellar-cortex development extends approximately between postnatal day 8 (P8) and P24 (Altman and Bayer 1997; Gramsbergen 1993), and has been shown vulnerable to various insults with lasting morphological and functional deficits (Altman and Bayer 1997; Bedi et al. 1980; Dobbing 1982). In the present study, we exposed rat pups to daily ETS (300, 100 and 0 $\mu g/m^3$ *TSP*) during the cerebellar vulnerable period, a rational initial point of investigation given its postnatal vulnerability and functional relevance to reported deficits and disorders. More broadly, this study addresses a lack of knowledge on neurobiological effects of ETS during development and studies potential mechanistic underpinnings.

METHODS

Animal procedures and tissue collection. Animals were treated humanely and with regard for alleviation of suffering. All procedures conformed to the U.S. Public Health Service policy with local Institutional Animal Care and Use Committee approval. Pregnant Sprague Dawley rats were purchased from Harlan Laboratories and housed in an AAALAC approved facility on a 12-h light cycle with ad libitum access to food and water. We treated male rat pups daily from age P8 to P23 in a Teague TE-10 smoking system operated as described previously by

us and others, with total suspended particulate (*TSP*) confirmed daily (Fuller et al. 2010; Gospe et al. 1996; Slotkin et al. 2001). The first of two exposure groups received amplified ETS at a mean daily level of 300 µg/m^3 *TSP* (ETS_{300}), with peak concentrations at 2 mg/m^3 during active smoking. The extreme concentration modeled here is realistic to ETS in cars (Ott et al. 2008), and was used to more readily detect a biochemical response in our initial mechanistic studies. Exaggerated chronic exposure may also be considered relevant for ETS exposure in combination with urban pollution, where mean daily *TSP* levels can measure in large metropolitan areas in the 100's µg/m^3 principally from other combustion sources (Calderon-Garciduenas et al. 2008). In a second exposure we modeled upper quartile ETS levels found in homes with smokers, with a mean daily level of 100 µg/m^3 *TSP* (ETS_{100}) peaking at 0.5 mg/m^{3}during active smoking (U.S. Environmental Protection Agency 1992). This exposure approximated ETS levels recorded from bedrooms of pre-school children in homes with a pack-a-day smoker (McCormack et al. 2008). Litters cumulatively received 3 h/day of exposure, apart from dams, with feedings in between. Control animals were handled identically except for not receiving ETS exposure. Mean daily carbon monoxide levels remained below 5 ppm. Animal weight was monitored daily and no difference was found between groups. Brains were collected after the close of the initial cerebellar vulnerability period at P25.

Locomotor activity. Using previously described procedures with the following modifications, we measured spontaneous locomotor activity in an unfamiliar environment at P25 during the light cycle (11am – 2pm) (Stohr et al. 1998). Animals were placed in a 42x42x30 cm^3 open field arena under red light illumination (1 lux at height of animal). Chambers were located within a sound isolated room. ETS_{100} exposed and one control (Cnt) group received acute saline (1 mL/kg, ip, Sal) while a second hyperlocomotor positive control group received acute

amphetamine (1 mg/kg, ip, Amp): ETS/Sal, Cnt/Sal, Cnt/Amp. We placed animals in the center of the arena 15 min after injection and recorded activity (total distance traveled, maximum velocity and entries into a 14x14 cm^2 central zone) assessed in 1-min intervals using ANY-maze tracking software (v.4.84, Stoelting, Wood Dale, IL). We cleaned the arena with 90% ethanol with the odor blown off prior to subsequent testing. The 1 mg/kg amphetamine dose was based on our pilot data indicating increase locomotor activity without stereotypic behavior. In contrast, both increase locomotion and stereotypic behavior were observed at 3 mg/kg (data not shown).

Two-dimensional chromatography-tandem mass spectrometry. Tissue from cerebellar hemisphere was processed through a multistep protein extraction procedure described previously (Cortes et al. 2012). Briefly, we sequentially homogenized tissue in aqueous (Matrix Extract) and membrane dissociation buffers (Membrane Extract) to resolve the neuroproteome into matrix-associated and membrane-associated compartments (Cortes et al. 2012). We assayed protein concentration with a Pierce660 kit (Thermo Scientific, Rockford, IL). 50 µg protein samples were reduced, alkylated, trypsin digested and concentrated into 20 µL of 100 mM ammonium formate (pH 10). We injected protein digests (4 µL ea.) in a treatment-interspersed order onto a two-dimensional nanoACQUITY UPLC system using an On-Line RP/RP 2D Separations kit ahead of a Synapt HDMS mass spectrometer operated in a data-independent acquisition mode (Waters, Milford, MA). We used Waters PLGS software (v.2.4) to process and annotate mass spectral data (Uniprot KB Rattus database). We filtered peptide annotations to a 1% false positive identification rate. For label-free quantification, we tabulated all unique peptides from Matrix and Membrane Extracts with their chromatographic peak area intensities across all biological replicates (n=8). Data were log(2) transformed, normalized and imputed for non-random missing values (for more detail, see Supplemental Material).

***Interaction informatics*.** Peptide measures found statistically responsive to ETS exposure reflected putative modulation of a parent protein or protein family's abundance, modification or localization. We performed protein enrichment analysis against GO annotation terms (biochemical process and cellular component) and biochemical pathways using a Fisher's inverse chi-square method with Bonferroni correction (ToppGene, initial alpha 0.05) (Chen et al. 2009). Further detail on enriched pathways was assessed through the KEGG Pathway Database (Kanehisa et al. 2010). Proteins associated with the GO term Mitochondrion (GO:0005739), the most significant enriched cellular component, were analyzed further using protein-protein network analysis (STRING Ver. 8.3, (Szklarczyk et al. 2011)) with the following parameters: a minimum interaction confidence score of 0.5, ≤ 10 interactors and displayed in evidence view applying MCL clustering.

***Immunoblot analysis*.** We resolved protein-balanced samples (10 μg) using the NuPAGE gel system, 4–12% Bis-Tris gels and MOPS running buffer (Life Technologies, Grand Island, NY), and transferred to PVDF membrane (Millipore, Billerica, MA) via a semi-dry method using NuPAGE transfer buffer (Life Technologies). We then probed the membrane with one of the following primary antibodies: anti-mouse hexokinase-1 (Sigma-Aldrich, St. Louis, MO), anti-mouse ATP synthase 5A (Abcam, Cambridge, MA), anti-rabbit dynamin-1-like protein (Origene, Rockville, MD). We used IgG HRP-conjugated secondary antibodies and the SuperSignal West Pico chemiluminescence detection kit (Thermo Scientific) for imaging. Blots were re-probed with anti-mouse beta-actin (Abcam) for controlling load error. We acquired 16-bit blot images on an Image Station 4000MM Pro CCD imager and measured net band intensity (Carestream Health, Rochester, NY).

Immunofluorescence microscopy. Cerebellar hemisphere tissues were sagitally cryosectioned (10 µm, sagittal) from 2 to 2.25 mm lateral of midline and fixed with 3% paraformaldehyde. Sections were probed with anti-mouse mitofilin (MitoSciences, Eugene, OR), anti-rabbit dynamin-1-like (Origene), and anti-rabbit Calbindin1 (Swant, Marly, Switzerland). We used Alexa Fluor conjugated secondary antibodies (Life Technologies) to acquire at least four images per lamina in lobule VIII from four sections on a Zeiss AxioImager A1 fluorescence microscope utilizing identical parameters. Images were analyzed blind to treatment with relative fluorescent intensity measured for regions of interest in ImageJ (Abramoff et al. 2004).

Transmission electron microscopy. Additional sagittal sections from ETS and control tissues described above were collected at a 50 µm thickness. We fixed with 2% glutaraldehyde, 2% paraformaldehyde (60 min at 4°C) and post-fixed in 1% osmium tetroxide (2 h). Afterwards, we dehydrated the sections through a graded ethanol series (50% to 100%), transitioned through propylene oxide and then infiltrated overnight in Embed 812 (Electron Microscopy Sciences, Hatfield, PA). We collected thin sections (80 nm) by ultramicrotomy onto copper 300 mesh thin bar grids and contrasted in lead citrate and uranyl acetate. We used a Jeol JEM-1230 transmission electron microscope to collect digital micrographs. Morphometric stereological analysis of mitochondria was performed about the medial neurpil of cerebellar molecular layer (Gosker et al. 2007; Siskova et al. 2010). Measurements included the mitochondrial fractional area (FA), the mean mitochondrial profile area (MA), and the mean number of mitochondria per area (MD). Mitochondrial profiles were counted and encircled when falling within a counting frame grid placed sequential-randomly five times per section as optimized from pilot images to measure between 100 and 200 mitochondria per animal (Mouton 2002). We also assessed

mitochondrial structure among sub-populations localized within processes and soma of Purkinje, granular and glial cells.

Statistical analysis. We evaluated locomotor activity using GLM multivariate testing and least significant difference post-hoc comparisons (α=0.05) in SPSS (v.20). We used one-way ANOVA testing on normalized neuroproteomic data using DanteR software (see Supplemental Material). We corrected for multiple peptide measures using the Benjamini-Yekutieli FDR method to control type 1 error to 5% (Benjamini and Yekutieli 2001). We load normalized immunoblot data in ratio to corresponding beta-actin data. Immunoblot and microscopy data were tested using either a Student's *t*-test method or a two-way ANOVA with the Holm-Sidak method (α=0.05).

RESULTS

Heightened activity with ETS exposure during postnatal cerebellar development. Our model of ETS exposure resulted in heightened locomotor activity in a novel environment. We found a significant main effect of ETS exposure for measures of distance traveled ($F_{1,28}$=26.49, p=1.9e^{-5}), maximum velocity ($F_{1,28}$=8.7, p=0.006) and entries into the center zone of the test arena ($F_{1,28}$=6.5, p=0.017). Figure 1 displays the time course of habituation to the novel environment and representative locomotor track plots for each group. Post-hoc comparisons across time are illustrated as significantly different between ETS_{100} exposed animals (ETS/Sal) relative to a matched air exposed group (Cnt/Sal) as well as an air exposed group stimulated with amphetamine (1 mg/kg, Cnt/Amp). We used the Cnt/Amp group as a positive control for a heightened locomotor response, which, as expected, maintained a higher asymptotic level of locomotor activity during and following habituation. Our data reveal that ETS/Sal animals when

placed in a novel environment initially exhibited a locomotor phenotype resembling that of Cnt/Amp stimulated animals. While ETS/Sal animals were more reactive (more locomotion) to a novel environment than Cnt/Sal animals, they eventually achieved the same baseline as Cnt/Sal animals during the second half of the session.

ETS induces underlying cerebellar mitochondrial subproteome perturbation and upregulates aerobic respiration machinery. To begin to understand the neurodevelopmental effects of ETS exposure and underlying mechanisms of action, we employed unbiased proteomic analysis in a systems biology approach. Bioinformatic assessment (see Supplemental Material, Figure S1) of neuroproteomic change following daily ETS_{300} exposure revealed 662 responsive peptide measures (Figure 2A) that denoted translational and post-translational dynamics among 389 proteins. This ETS-responsive neuroproteome particularly overrepresented change to the mitochondrial subproteome (103 proteins representing 28% of Mitochondrion GO term GO:0005739, p=5.33e-29). All three major aerobic respiration pathways responded to ETS exposure (Figure 2B). This included significant modulation of all glycolytic enzymes, 16 proteins involved in downstream pyruvate processing (e.g., 5 of 8 tricarboxylic acid cycle enzymes) and 10 subunits of 4 electron transport chain complexes (see Supplemental Material, Figure S2). These data revealed that ETS exposure during cerebellar-cortex development prominently influenced mitochondria and in particular processes involved in aerobic function.

We next assessed the regulational state of aerobic metabolism, which is governed by post-translational dynamics of the rate-limiting enzyme hexokinase 1 (Hk1). Hk1 peptide measures (Figure 2C) indicated a treatment-induced shift in localization. Mass spectrometry also revealed three previously unknown phosphorylated and glycosylated Hk1 motifs that were responsive to ETS_{300} exposure (Hk1 - Modified Peptides Figure 2C, see Supplemental Material,

Figure S3). We further affirmed that Hk1 translocation was dose-dependent with 45% and 22% shifts to the mitochondrial membrane relative to controls following ETS_{300} and ETS_{100} exposures, respectively (Figure 2D). We also observed an ETS_{300} induced increased in peptide levels of ATP synthase (ATP5) (Figure 2E), which exhibited a dose-dependent 51% or 23% response to ETS_{300} and ETS_{100} exposures, respectively, over matched controls (Figure 2F).

ETS stimulates Dnm1l mitochondrial fission independent of stress-induced Bcl2 family dynamics. We examined whether the significant upregulation of aerobic respiration machinery co-occurred with altered mitochondrial fission/fusion dynamics. The ETS-responsive neuroproteome revealed significant modulation of the mitochondrial fission factor dynamin-1-like protein (Dnm1l, a.k.a. Drp1) while the mitochondrial fusion factor mitofusin was unresponsive to ETS exposure. Dnm1l peptide measures reflected a significant increase with ETS_{300} exposure (Figure 3A). We further measured 35% less phosphorylation at S_{615} (S_{596} in human) relative to control (p=0.026) by tandem mass spectrometry (Figure 3B). After ETS_{300} exposure, we measured a robust 125% increase in cytosolic Dnm1l; however, a lower 53% increase in mitochondria-bound Dnm1l did not reach significance at p=0.15 (Figure 3C). In sharp contrast, the milder ETS_{100} exposure induced a dramatic 311% increase in active membrane-bound Dnm1l over controls, while the 32% increase in cytosolic Dnm1l was more in line with a dose-dependent effect of exposure. We localized increased Dnm1l staining found more broadly distributed across molecular (ML) and Purkinje (PL) laminae of ETS_{100} exposed animals relative to controls (Figure 3D and D', respectively). We further observed a corresponding increase in mitochondrial marker staining (MF), with Dnm1l-stained puncta found adjacent to MF stained mitochondria. We assayed Bcl-X_L levels, a known modulator of Dnm1l,

and a pro-apoptotic Bcl-2 family member, Bcl-2 binding component 3; however, both were found unchanged with ETS exposure (Figure 3E).

ETS induces mitochondrial biogenesis, not fragmentation, in cerebellar-cortex. We further evaluated the extent and nature of Dnm1l-mediated mitochondrial fission. As previously shown with ETS_{100} exposure, ETS_{300} exposure significantly increase mitofilin stained mitochondria within the ML and PL (Figure 4A). In contrast, GL mitochondrial staining was also heightened with ETS_{300} exposure. Mean immunofluorescence intensity was significantly greater in all three laminae (Figure 4B), with the greatest increase relative to control in the ML. To explore whether these results were consequent to an increase in mitochondrial fragmentation (degeneration), increased network size or biogenesis we examined mitochondrial morphology by electron microscopy. From morphometric stereological analysis, we affirmed that the fractional area occupied by mitochondria in the ML doubled with ETS_{300} exposure relative to controls (Figures 4D,D'), which closely agreed with our immunofluorescence data. The mean profile area, an indication of mitochondrial size, showed no statistical difference between groups; whereas, the count of mitochondrial profiles per field was significantly greater at double that of control. Qualitative assessment of micrographs localized the greater mitochondrial density particularly to Purkinje dendrites in the ML of ETS exposed animals relative to controls (Figures 4C,C'). Yet, mitochondrial ultrastructure remained consistent and healthy appearing between groups (Figure 4E,E'), with no distinguishable morphological difference from control to suggest stress-induced fragmentation across neuronal and glial subpopulations within the GL, PL and ML (see Supplemental Material, Figure S4).

DISCUSSION

Presented are the first findings to our knowledge demonstrating a significant effect of postnatal ETS exposure on behavior and a potential underlying mechanism involving perturbed mitochondrial energetics critical to the developing brain. This novel insight into the pathobiological impact of ETS during a vulnerable period is the product of a systems biology approach using unbiased proteomic assessment. Prenatal maternal exposure to cigarette smoke has been well documented to induce neurological as well as many other lasting health effects as reviewed elsewhere (Doherty et al. 2009; Pauly and Slotkin 2008). Yet, very few studies have explored neurobiological effects relevant to postnatal ETS exposure, despite mounting evidence for adverse behavioral and cognitive outcomes. Thus, we believe results from this study represent a significant advance in the limited knowledge affirming neurobehavioral and neurobiological effect of ETS exposure during development.

Cerebellar perturbation can broadly impact regulation of behavioral and cognitive domains (Steinlin 2008). Results here show that animals exposed to ETS during postnatal cerebellar development exhibited heightened locomotor activity in a novel environment with a slower rate of habituation relative to controls. The initial heightened locomotor response of the ETS/Sal group was remarkably similar to that of animals injected with a moderate amphetamine dose (Cnt/Amp). These findings were observed across three different dependent measures for the first half of the session. Further, ETS/Sal animals were slower to habituate than either control group, but reached a similar baseline activity to Cnt/Sal animals during the last half of the session. These data suggest an increased response and diminished ability to habituate to an unfamiliar open area rather than a persistent hyperlocomotor response as observed with amphetamine stimulation. Such a behavioral phenotype might result from an ETS-mediated perturbation of inhibitory control loops between cerebellum and neocortex that govern action

control (Altman and Bayer 1997). Altman and colleagues demonstrated that late perturbation during the rat cerebellar vulnerable period, as studied here for ETS, selectively induced (potentially hazardous) heightened activity by impacting late ML synaptic development. These findings stand in contrast to generalized mobility deficits seen with cell loss following early cerebellar insult.

The functional deficits seen in ETS exposed children suggest perturbation to circuits involving multiple brain regions, and indeed we previously observed change in frontal cortex, hippocampus and cerebellum following modeled adult ETS exposure (Fuller et al. 2010). However, the mechanistic studies here warranted anatomical focus. Cerebellar development was a rational point of investigation given extended postnatal vulnerability and relevance to deficits and disorders impacted by ETS exposure in children. Interestingly, Gospe et al. in the first neurobiological study to model postnatal ETS exposure showed a greater effect in hindbrain over forebrain suggesting cerebellar susceptibility (Gospe et al. 1996). Present findings affirm a significant neurobiological effect of postnatal ETS exposure on cerebellum including at household relevant levels. We further identified perturbed mitochondrial energetics as an underlying mechanism that is significant given the correlation to neuronal activity (Kann and Kovacs 2007).

Aerobic demands increase postnatally with heighted synaptic development, requiring more ATP to maintain membrane polarity. Our results show that developmental ETS exposure perturbed mitochondria and associated aerobic pathways. Hk1 is a key regulator of aerobic ATP production, governed by dynamic recruitment from the cytosol to the mitochondrial membrane (de Cerqueira Cesar and Wilson 2002). Our data reveal a dose-dependent shift in Hk1 to the mitochondrial membrane with ETS exposure. Hk1 translocation involves a positive-feedback

mechanism with ATP5 utilizing yet unknown post-translational signaling to alter Hk1 conformation and binding (Hashimoto and Wilson 2000; Pastorino and Hoek 2008). Our results show a corresponding dose-dependent increase in ATP5 and modification of three previously unreported Hk1 post-translational motifs in response to ETS exposure. Indeed, these modification sites may be found to govern Hk1 dynamics under aerobic respiration with future research.

Brain energetics is further regulated through mitochondrial fission/fusion dynamics. The ETS-responsive neuroproteome reveals significant upregulation and modification of fission factor Dnm1l. Predominantly in the cytosol, Dnm1l initiates fission when recruited to the mitochondrial membrane following post-translational modification (Baloh 2008; Berman et al. 2008; Uo et al. 2009). Dnm1l was significantly dephosphorylated at S_{615}, a motif believed to inhibit function; i.e., Dnm1l activity is disinhibited following ETS exposure (Corradino and De Palma 2011; De Palma et al. 2010). Greater Dnm1l stained puncta were found localized with mitochondria particularly within the ML with localization to Purkinje dendrites observed by EM. Heightened ML plasticity critical to cerebellar function remains ongoing through childhood on into adolescence (Tiemeier et al. 2010). Interestingly, Li et al. reported Dnm1l involvement in synaptogenesis as well as mitochondrial biogenesis during development (Li et al. 2008). Findings here may also correlate or perhaps compensate for ETS-altered maladaptive synaptogenesis given the close relationship between mitochondrial energetics and synaptogenesis and plasticity in the brain. Thus, the relationship between Dnm1l-mediated mitochondrial biogenesis and aberrant synaptic formation or function following ETS exposure warrants future exploration.

Results of this study also refute the alternative of oxidative stress induced mitochondrial fragmentation, which too is mediated by Dnm1l. Cigarette smoke is well known to induce oxidative stress in other organs to result in mitochondrial dysfunction and a pro-apoptotic environment involving Bcl-2 family signaling (Armani et al. 2009; Westbrook et al. 2010). In particular, Bcl-X_L binds and activates Dnm1l fission under oxidative-stress conditions (Wu et al. 2011). Yet, our results demonstrate that Bcl-X_L is unresponsive to ETS exposure. Likewise, ETS exposure did not affect levels of pro-apoptotic Bcl-2 binding component 3. Mitochondrial structure appeared undisturbed with ultrastructural analysis. The ETS-responsive neuroproteome lacked a significant association with oxidative stress or apoptotic pathways. Moreover, oxidative stress is known to reduce aerobic respiration, which contrasted with our finding of upregulated aerobic processes. Together, these results support that Dnm1l activation occurs independent of stress-induced Bcl-2 family dynamics and that mitochondrial fragmentation is not occurring in cerebellum after ETS exposure.

Importantly, we found a dose-dependency in the biochemical response to ETS exposure. Most measured change was halved in response to a 3-fold reduction in ETS levels. These data suggest that a further 3-fold reduction in ETS exposure could still result in a significant effect assuming a linear relationship, which suggests relevance across a majority of household exposure. Critically, our results show a greater increase in active mitochondrion-tethered Dnm1l following lower ETS_{100} exposure relative to control despite lower overall expression of the protein relative to ETS_{300} exposure. Future studies are needed to demonstrate an effect at lower level or low incidence ETS exposure. Also of importance is the interaction between ETS and chronic urban air pollution given prevalent co-exposure. Recently, Calderón-Garcidueñas et al. showed that severe (heightened *TSP*) urban air pollution is also a risk factor for attention,

language and learning cognitive deficits suggesting potential for a synergistic effect (Calderon-Garciduenas et al. 2011).

CONCLUSION

In summary, ETS exposure modeled during the postnatal vulnerable period of cerebellar development resulted in a behavioral phenotype and underlying perturbation to mitochondrial energetics in cerebellum that suggest an effect on action control. Our findings further support a biological mechanism involving perturbation to Dnm1l-mediated mitochondrial proliferation during critical postnatal cerebellar development, which presents an opportunity for pharmacological intervention. Ongoing cerebellar development, particularly in the molecular layer, is dependent on tight regulation of mitochondrial dynamics. Our data affirm an association of increased Dnm1l activity with mitochondrial biogenesis rather than fragmentation mediated through Bcl-2 family regulation under oxidative-stress. Findings here may also have broader implications for other environmental exposures, given that ETS is comprised of a wide range of toxic chemicals, heavy metals and combustion particulate matter, and other neuropsychiatric conditions. More recently, cerebellar dysfunction is also being recognized as involved in schizophrenia and autism (O'Halloran et al. 2012). All together, these findings represent a significant contribution to the limited knowledge on neurodevelopmental effects of ETS exposure, and emphasize a mechanism of action involving cerebellar perturbation. These findings further encourage efforts to eliminate children's exposure to ETS by revealing a plausible biological link with mental health disorders. Results here also support therapeutic

potential targeting mitochondrial dynamics to treat ETS-induced neurobehavioral and cognitive deficits that impact long-term quality of life.

REFERENCES

Abramoff MD, Magalhaes PJ, Ram SJ. 2004. Image processing with ImageJ. Biophotonics Int 11:36-42.

Aguiar A, Eubig PA, Schantz SL. 2010. Attention deficit/hyperactivity disorder: A focused overview for children's environmental health researchers. Environ Health Perspect 118:1646-1653.

Altman J, Bayer SA. 1997. Development of the Cerebellar System: In Relation to its Evolution, Structure, and Functions. Boca Raton, FL:CRC Press.

Anderko L, Braun J, Auinger P. 2010. Contribution of tobacco smoke exposure to learning disabilities. J Obstet Gynecol Neonatal Nurs 39:111-117.

Armani C, Landini L,Jr, Leone A. 2009. Molecular and biochemical changes of the cardiovascular system due to smoking exposure. Curr Pharm Des 15:1038-1053.

Baloh RH. 2008. Mitochondrial dynamics and peripheral neuropathy. Neuroscientist 14:12-18.

Bandiera FC, Richardson AK, Lee DJ, He JP, Merikangas KR. 2011. Secondhand smoke exposure and mental health among children and adolescents. Arch Pediatr Adolesc Med 165:332-338.

Bedi KS, Hall R, Davies CA, Dobbing J. 1980. A stereological analysis of the cerebellar granule and purkinje cells of 30-day-old and adult rats undernourished during early postnatal life. J Comp Neurol 193:863-870.

Benjamini Y, Yekutieli D. 2001. The control of the false discovery rate in multiple testing under dependency. Ann Stat 29:1165-1188.

Berman SB, Pineda FJ, Hardwick JM. 2008. Mitochondrial fission and fusion dynamics: The long and short of it. Cell Death Differ 15:1147-1152.

Bledsoe JC, Semrud-Clikeman M, Pliszka SR. 2011. Neuroanatomical and neuropsychological correlates of the cerebellum in children with attention-deficit/hyperactivity disorder-combined type. J Am Acad Child Adolesc Psychiatry 50:593-601.

Calderon-Garciduenas L, Engle R, Mora-Tiscareno A, Styner M, Gomez-Garza G, Zhu H et al. 2011. Exposure to severe urban air pollution influences cognitive outcomes, brain volume and systemic inflammation in clinically healthy children. Brain Cogn 77:345-355.

Calderon-Garciduenas L, Solt AC, Henriquez-Roldan C, Torres-Jardon R, Nuse B, Herritt L et al. 2008. Long-term air pollution exposure is associated with neuroinflammation, an altered innate immune response, disruption of the blood-brain barrier, ultrafine particulate deposition, and accumulation of amyloid beta-42 and alpha-synuclein in children and young adults. Toxicol Pathol 36:289-310.

Centers for Disease Control and Prevention. 2010.
Vital signs: Nonsmokers' exposure to secondhand Smoke—United states, 1999–2008. MMWR 59:1135-1140.

Chen J, Bardes EE, Aronow BJ, Jegga AG. 2009. ToppGene suite for gene list enrichment analysis and candidate gene prioritization. Nucleic Acids Res 37:W305-W311.

Colman GJ, Joyce T. 2003. Trends in smoking before, during, and after pregnancy in ten states. Am J Prev Med 24:29-35.

Corradino R, De Palma C. 2011. PKG is the new regulator of Drp1 function. In: 35 Congresso Nazionale della Societa Italiana di Farmacologia, September 14-17, Bologna, Italy:Societa Italiana di Farmacologia.

Cortes DF, Landis MK, Ottens AK. In press. High-capacity peptide-centric platform to decode the prtoeomic response to brain injury. Electrophoresis.

Dalwani M, Sakai JT, Mikulich-Gilbertson SK, Tanabe J, Raymond K, McWilliams SK et al. 2011. Reduced cortical gray matter volume in male adolescents with substance and conduct problems. Drug Alcohol Depend 118:295-305.

de Cerqueira Cesar M, Wilson JE. 2002. Functional characteristics of hexokinase bound to the type a and type B sites of bovine brain mitochondria. Arch Biochem Biophys 397:106-112.

De Palma C, Falcone S, Pisoni S, Cipolat S, Panzeri C, Pambianco S et al. 2010. Nitric oxide inhibition of Drp1-mediated mitochondrial fission is critical for myogenic differentiation. Cell Death Differ 17:1684-1696.

Dobbing J. 1982. The later development of the brain and its vulnerability. In: Scientific Foundations of Paediatrics (Davis JA, Dobbing J, eds) . Baltimore:University Park Press, 744-759.

Doherty SP, Grabowski J, Hoffman C, Ng SP, Zelikoff JT. 2009. Early life insult from cigarette smoke may be predictive of chronic diseases later in life. Biomarkers 14 Suppl 1:97-101.

Friede RL. 1973. Dating the development of human cerebellum. Acta Neuropathol 23:48-58.

Fuller BF, Gold MS, Wang KK, Ottens AK. 2010. Effects of environmental tobacco smoke on adult rat brain biochemistry. J Mol Neurosci 41:165-171.

Gosker HR, Hesselink MK, Duimel H, Ward KA, Schols AM. 2007. Reduced mitochondrial density in the vastus lateralis muscle of patients with COPD. Eur Respir J 30:73-79.

Gospe SM,Jr, Zhou SS, Pinkerton KE. 1996. Effects of environmental tobacco smoke exposure in utero and/or postnatally on brain development. Pediatr Res 39:494-498.

Gramsbergen A. 1993. Consequences of cerebellar lesions at early and later ages: Clinical relevance of animal experiments. Early Hum Dev 34:79-87.

Hashimoto M, Wilson JE. 2000. Membrane potential-dependent conformational changes in mitochondrially bound hexokinase of brain. Arch Biochem Biophys 384:163-173.

Kabir Z, Connolly GN, Alpert HR. 2011. Secondhand smoke exposure and neurobehavioral disorders among children in the united states. Pediatrics 128:263-270.

Kanehisa M, Goto S, Furumichi M, Tanabe M, Hirakawa M. 2010. KEGG for representation and analysis of molecular networks involving diseases and drugs. Nucleic Acids Res 38:D355-D360.

Kann O, Kovacs R. 2007. Mitochondria and neuronal activity. Am J Physiol Cell Physiol 292:C641-57.

Koop M, Rilling G, Herrmann A, Kretschmann HJ. 1986. Volumetric development of the fetal telencephalon, cerebral cortex, diencephalon, and rhombencephalon including the cerebellum in man. Bibl Anat 28:53-78.

Li H, Chen Y, Jones AF, Sanger RH, Collis LP, Flannery R et al. 2008. Bcl-xL induces Drp1-dependent synapse formation in cultured hippocampal neurons. Proc Natl Acad Sci U S A 105:2169-2174.

Marano C, Schober SE, Brody DJ, Zhang C. 2009. Secondhand tobacco smoke exposure among children and adolescents: United states, 2003-2006. Pediatrics 124:1299-1305.

McCormack MC, Breysse PN, Hansel NN, Matsui EC, Tonorezos ES, Curtin-Brosnan J et al. 2008. Common household activities are associated with elevated particulate matter concentrations in bedrooms of inner-city baltimore pre-school children. Environ Res 106:148-155.

Mouton PR. 2002. Principles and Practices of Unbiased Stereology: An Introduction for Bioscientists. Baltimore:John Hopkins University Press.

Oberg M, Jaakkola MS, Woodward A, Peruga A, Pruss-Ustun A. 2011. Worldwide burden of disease from exposure to second-hand smoke: A retrospective analysis of data from 192 countries. Lancet 377:139-146.

O'Halloran CJ, Kinsella GJ, Storey E. 2012. The cerebellum and neuropsychological functioning: A critical review. J Clin Exp Neuropsychol 34:35-56.

Ott W, Klepeis N, Switzer P. 2008. Air change rates of motor vehicles and in-vehicle pollutant concentrations from secondhand smoke. J Expo Sci Environ Epidemiol 18:312-325.

Pastorino JG, Hoek JB. 2008. Regulation of hexokinase binding to VDAC. J Bioenerg Biomembr 40:171-182.

Pauly JR, Slotkin TA. 2008. Maternal tobacco smoking, nicotine replacement and neurobehavioural development. Acta Paediatr 97:1331-1337.

Richter S, Dimitrova A, Hein-Kropp C, Wilhelm H, Gizewski E, Timmann D. 2005. Cerebellar agenesis II: Motor and language functions. Neurocase 11:103-113.

Siskova Z, Mahad DJ, Pudney C, Campbell G, Cadogan M, Asuni A et al. 2010. Morphological and functional abnormalities in mitochondria associated with synaptic degeneration in prion disease. Am J Pathol 177:1411-1421.

Slotkin TA, Pinkerton KE, Garofolo MC, Auman JT, McCook EC, Seidler FJ. 2001. Perinatal exposure to environmental tobacco smoke induces adenylyl cyclase and alters receptor-mediated cell signaling in brain and heart of neonatal rats. Brain Res 898:73-81.

Steinlin M. 2008. Cerebellar disorders in childhood: Cognitive problems. Cerebellum 7:607-610.

Stohr T, Schulte Wermeling D, Weiner I, Feldon J. 1998. Rat strain differences in open-field behavior and the locomotor stimulating and rewarding effects of amphetamine. Pharmacol Biochem Behav 59:813-818.

Szklarczyk D, Franceschini A, Kuhn M, Simonovic M, Roth A, Minguez P et al. 2011. The STRING database in 2011: Functional interaction networks of proteins, globally integrated and scored. Nucleic Acids Res 39:D561-D568.

Tiemeier H, Lenroot RK, Greenstein DK, Tran L, Pierson R, Giedd JN. 2010. Cerebellum development during childhood and adolescence: A longitudinal morphometric MRI study. Neuroimage 49:63-70.

U.S. Department of Health and Human Services. 2006. The health consequences of involuntary exposure to tobacco smoke: A report of the surgeon general. O2NLM: WA 754 H4325 2006. Atlanta, GA:U.S. Surgeon General.

U.S. Environmental Protection Agency. 1992. Respiratory health effects on passive smoking: Lung cancer and other disorders. Publication # 600/6-90/006F. Washington, DC.

Uo T, Dworzak J, Kinoshita C, Inman DM, Kinoshita Y, Horner PJ et al. 2009. Drp1 levels constitutively regulate mitochondrial dynamics and cell survival in cortical neurons. Exp Neurol 218:274-285.

Valera EM, Faraone SV, Murray KE, Seidman LJ. 2007. Meta-analysis of structural imaging findings in attention-deficit/hyperactivity disorder. Biol Psychiatry 61:1361-1369.

Westbrook DG, Anderson PG, Pinkerton KE, Ballinger SW. 2010. Perinatal tobacco smoke exposure increases vascular oxidative stress and mitochondrial damage in non-human primates. Cardiovasc Toxicol 10:216-226.

Wu S, Zhou F, Zhang Z, Xing D. 2011. Mitochondrial oxidative stress causes mitochondrial fragmentation via differential modulation of mitochondrial fission-fusion proteins. FEBS J 278:941-954.

FIGURE LEGENDS

Figure 1. Spontaneous locomotor activity is increased following postnatal ETS exposure. Following initial rat cerebellar-cortex formation, locomotor activity in a 42x42x30 cm^3 open field was recorded at P25 for ETS_{100} exposed or plain air control (Cnt) animals. Amphetamine (Amp; 1 mg/kg) as hyperlocomotion positive control or saline vehicle (Sal) was injected (ip) 15 min prior. (*A*) Plot of total distance traveled quantified in 1-min bins. (*B*) Plot of maximum velocity quantified in 1-min bins. (*C*) Representative locomotor track plots for animals with a median measure of total distance traveled per treatment group; 14x14 cm^2 central zone shown boxed. (*D*) Plot of entries into the central zone quantified in 1-min bins. Values reported as Mean±SE; n=14/group; * $p<0.05$ ETS/Sal compared to Cnt/Sal; $^{++}p<0.05$ ETS/Sal compared to Cnt/Amp.

Figure 2. Significant cerebellar proteome perturbation following ETS exposure with dose-dependent upregulation of aerobic processes. Animals were exposed daily to ETS or plain air (Cnt). (*A*) Quantitative proteomics revealed 662 responsive peptides to ETS_{300} exposure in cerebellar-cortex, denoting significant change among 389 proteins. Fold change; n=4/group; corrected $\alpha=0.0049$. (*B*) Aerobic respiration pathways prominently altered in the ETS-responsive neuroproteome. % pathway coverage; corrected $\alpha=0.016$. Heatmap plots of ETS_{300} responsive peptide measures for (*C*) Hk1 (unmodified and post-translationally modified) and (*E*)ATP5 . (Log2, ratio to control; n=4/group; p-values reported). Dose-dependent immunoblot protein measures of (*D*) Hk1 and (*F*) ATP5a. Cytosolic (cyto.) and mitochondrial (mito.) protein levels graphed for Hk1 to assess subcellular translocation. Values reported as Mean±SE; n=4/group. *$p<0.05$ compared to controls. **$p<0.01$ compared across dose.

Figure 3. ETS stimulates Dnm1l-mediated mitochondrial fission independent of stress-induced Bcl2 family dynamics. Animals were exposed daily to two levels of ETS (300 µg/m3 or 100 µg/m3 TSP) or plain air (control). Heatmap of fission factor Dnm1l (*A*) unmodified peptide measures within the ETS-responsive neuroproteome and (*B*) tandem mass spectrum confirming reduced phosphorylation at S616 (Log2, ratio to control; n=4/group; ANOVA, p-value reported). Protein levels (*C*) of cytosolic (cyto.) and mitochondrial (mito.) Dnm1l were measured by immunoblot. Co-immunofluorescence staining of Dnm1l and the mitochondrial marker mitofilin (MF) in cerebellar-cortex of (*D*) ETS_{100} exposed and (*D'*) air control animals. Granular (GL), Purkinje (PL) and molecular (ML) laminae are demarked, and Dnm1l and MF channels are displayed separately on right. Bar=20 µm. Protein levels of (*E*) Bcl2-family members were measured by immunoblot analysis indicating no significant response to ETS exposure. Values reported as Mean±SE; n=4/group. *p<0.001 compared to controls. **p<0.001 compared across dose.

Figure 4. ETS induces Dnm1l-mediated mitochondrial biogenesis, not fragmentation, in cerebellar-cortex. The density of mitochondrial staining (MF) increased in (*A*) ETS_{300} exposed animals relative to (*A'*) air controls throughout cerebellar-cortex. Representative images; bar=20 µm (*A*); Purkinje cell staining magnified in inset. Mean MF immunofluorescence intensity (*B*) was significantly greater in granular layer (GL), Purkinje layer (PL) and molecular layer (ML) of cerebellar-cortex. Representative electron micrographs show more mitochondria within ML Purkinje dendrites (black arrows) of ETS exposed animals (*C*) relative to control (*C'*). Stereological measures of mitochondrial profiles (*D*) within the ML: mean mitochondrial fractional area (FA), mitochondrial profile area (MA), and mitochondrial density (MD). Mitochondrial ultrastructure appears healthy and consistent between ETS exposed (*E*) and

control (*E'*) animals. Representative images from the ML; bar=200 nm (*E*). Values reported as Mean±SE; n=4/group. *p<0.01 compared with controls.

Figure 1

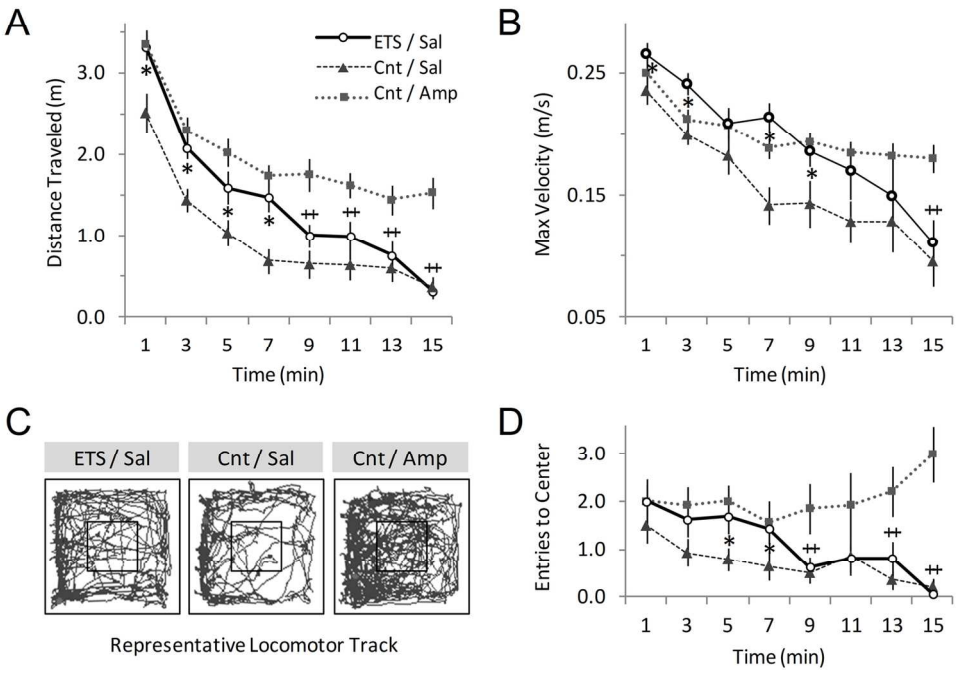

Figure 1. Spontaneous locomotor activity is increased following postnatal ETS exposure.
152x114mm (300 x 300 DPI)

Figure 2

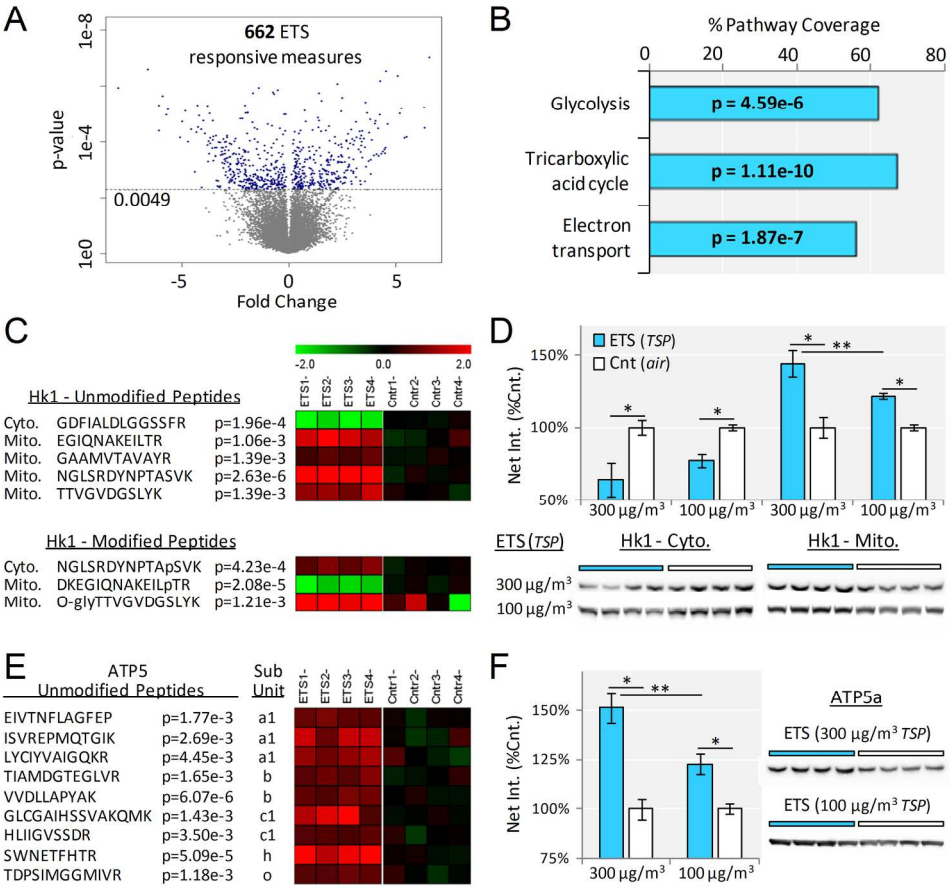

Figure 2. Significant cerebellar proteome perturbation following ETS exposure with dose-dependent upregulation of aerobic processes.
198x194mm (300 x 300 DPI)

Figure 3

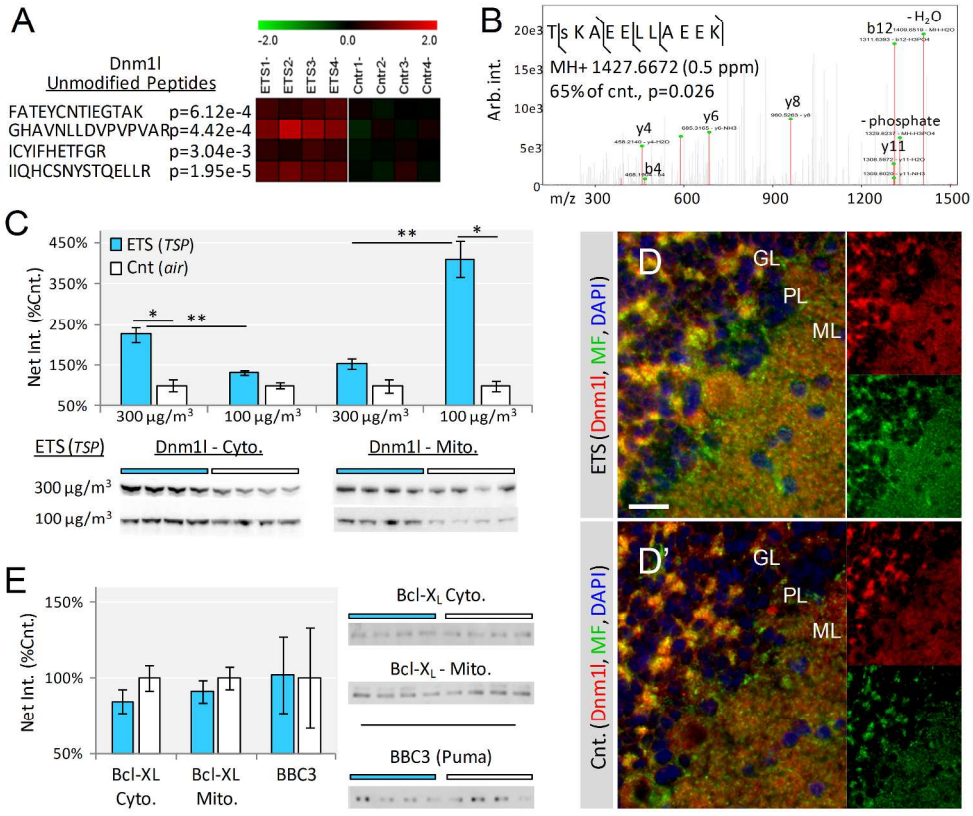

Figure 3. ETS stimulates Dnm1l-mediated mitochondrial fission independent of stress-induced Bcl2 family dynamics.
1287x1153mm (72 x 72 DPI)

Figure 4

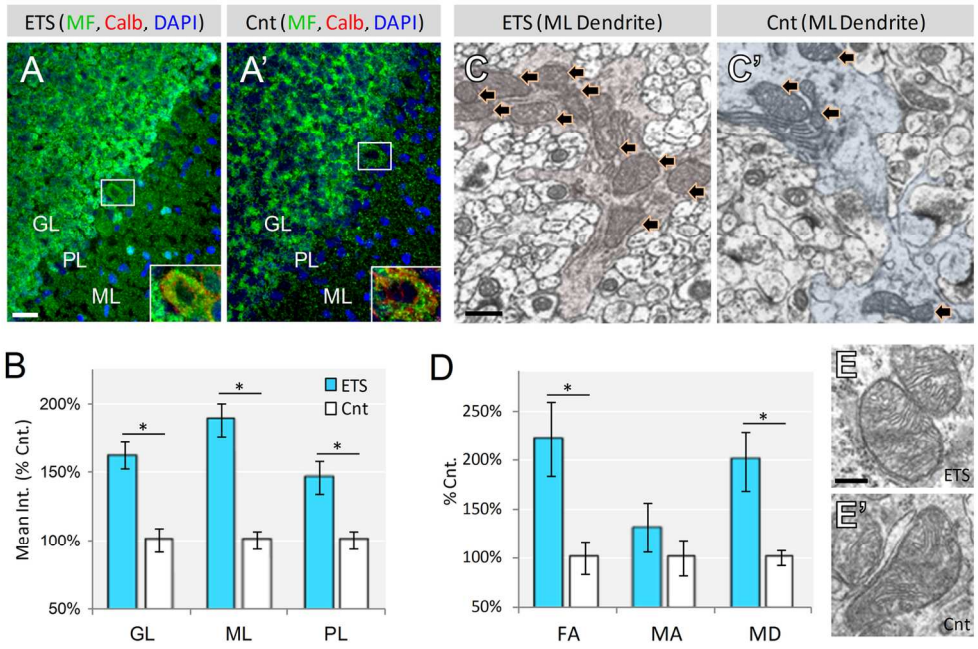

Figure 4. ETS induces Dnm1l-mediated mitochondrial biogenesis, not fragmentation, in cerebellar-cortex.
145x104mm (300 x 300 DPI)